Article

On the Phylogenetic Position of the Weevil Tribe Acentrusini Alonso-Zarazaga, 2005 (Coleoptera: Curculionidae: Curculioninae)

Michael Košťál [1,*] and Peter Vďačný [2]

1   Střelecká 459, 500 02 Hradec Králové, Czech Republic
2   Department of Zoology, Faculty of Natural Sciences, Comenius University in Bratislava,
    Mlynská dolina B-1, Ilkovičova 6, 842 15 Bratislava, Slovakia; peter.vdacny@uniba.sk
*   Correspondence: michael.kostal@iol.cz; Tel.: +420-606-729-022

Abstract: Based on intrinsic morphological and extrinsic bionomic characters, the systematic position of the weevil tribe Acentrusini Alonso-Zarazaga, 2005 (Coleoptera: Curculionidae: Curculioninae) was determined. Maximum parsimony and Bayesian inference as well as nonmetric multi-dimensional scaling were used to analyze 34 morphological characters of adults, complemented by four host plant characters associated with particular weevil tribes. Sixteen species belonging to two subfamilies (Brachycerinae, Curculionidae) and seven tribes (Acentrusini, Anthonomini, Ellescini, Erirhinini, Smicronychini, Storeini, Styphlini) of the family Curculionidae and one outgroup species (Attelabidae) were studied. Phylogenetic and multi-dimensional analyses revealed the tribe Smicronychini as most closely related to Acentrusini. Of the tribes of Curculioninae studied, Styphlini, Anthonomini and Ellescini showed a certain degree of phylogenetic relation to Acentrusini, whereas Storeini were found to be least related.

Keywords: Coleoptera; Curculionidae; Curculioninae; Acentrusini; phylogeny

1. Introduction

The tribe Acentrusini was described quite recently by Alonso-Zarazaga [1]. Until the description of two additional taxa [2], the tribe was monotypical and contained only *Cryptorhynchus histrio* Boheman, 1837, the type species of the genus *Acentrus*. *Acentrus histrio* (Boheman, 1837), *A. boroveci* (Košťál, 2014) and *A. zarathustra* (Košťál, 2014) are morphologically highly similar, apparently forming a monophyletic group [2]. Hence, the tribe is morphologically uniform, showing no subgeneric divergence and was characterized by Alonso-Zarazaga [1] by a body covered with densely arranged light scales; normal, horizontally movable mandibles with teeth on the inner side; antennae with seven funicular segments; eyes more close to each other on the ventral than on the dorsal part of the head; a lower rostrum margin in the lateral view directed to the middle of eye; postocular lobes on the anterior margin of the pronotum; prosternum with emargination; a precoxal distance twice as long as the metacoxal distance; ventrite 2 longer than ventrites 3–4 combined; the distance between metacoxae larger than the metacoxal width; free claws; and other, presumably apomorphic characters. The phylogenetic relation of Acentrusini has not yet been studied. Only Alsonso-Zarazaga [1] suggested a tentative hypothesis of their possible close relationship to Styphlini, without identifying any shared tribal characters. Later, some characters typical of Acentrusini, but also of other tribes, like ventrally contiguous eyes, were reported as descriptive characters without drawing phylogenetic affinities to Acentrusini [3]. The distribution of Acentrusini extends from the Iberian Peninsula and North Africa through the Mediterranean to southern Ukraine, Caucasus, the Middle East, Iran and

Turkmenistan. All known host plants belong to the family Papaveraceae. Alonso-Zarazaga [1] suspected that Acentrusini is most closely related to Styphlini, however noting the necessity of more detailed analysis of the phylogenetic relationships to this tribe.

2. Materials and Methods

2.1. Taxonomic and Morphological Methods

Sixteen weevil species from the family Curculionidae s. l., belonging to seven tribes, and one outgroup species from the family Attelabidae, tribe Rhynchitini (*Rhynchites bacchus* (Linnaeus, 1758)), were studied. Tribes of the subfamily Curculioninae from the Palaearctic region included in this study were selected based on published (Styphlini) [1] and unpublished assumed phylogenetic relationships to Acentrusini with respect to the morphological similarity to Acentrusini. Characters reported in the detailed redescription of Acentrusini as presumable apomorphies [1] were used as the tribe selection guideline. These characters include scales on the body (head and rostrum), dentation of the mandibles, the number of antennal funicle segments, the dorsal vs. ventral distance of eyes, the direction of the lower rostrum margin in relation to the eye, the presence or absence of postocular lobes and prosternal impression, the ratio of the precoxal and postcoxal distance and the medial length of ventrite 2 and ventrites 3–4 combined, and claw connation at the base [1]. As an additional important character, we consider here the venation of the hind wings. Of the 21 currently reported Palaearctic tribes of Curculioninae [4], only six meet to some extent a substantial part of the characters listed above. Those tribes that are generally not consistent with Acentrusini in most characters of higher taxonomic weight were not included. To support the validity of the phylogenetic tree, we also included three species of the subfamily Brachycerinae, tribe Erirhinini, which might remotely resemble Acentrusini in several plesiomorphies.

The taxonomy follows the latest higher taxonomical classification of Curculionoidea by Zarazaga et al. [4]. We included two subfamilies of Curculionidae, Brachycerinae Billberg, 1820 and Curculioninae Latreille, 1802, into the phylogenetic and multi-dimensional phenetic analyses. Brachycerinae were represented by the tribe Erirhinini Schoenherr, 1825, with the following species listed in alphabetical order: *Notaris scirpi* (Fabricius, 1772), *Thryogenes fiorii* Zumpt, 1928, and *T. scirrhosus* (Gyllenhal, 1835). Curculioninae were represented by the following tribes and species reported in brackets, both listed in alphabetical order: Acentrusini Alonso–Zarazaga, 2005 (*Acentrus histrio* (Boheman, 1837), *A. zarathustra* Košťál, 2014), Anthonomini C.G. Thomson, 1859 (*Anthonomus behnei* Košťál, 2014, *Bradybatus seriesetosus* Petri, 1912), Ellescini C.G. Thomson, 1859 (*Dorytomus taeniatus* (Fabricius, 1781), *Ellescus bipunctatus* (Linnaeus, 1758)), Smicronychini Seidlitz, 1891 (*Smicronyx jungermanniae* (Reich, 1797), *S. reichii* (Gyllenhal, 1835), *Sharpia* sp.), Storeini Lacordaire, 1863 (*Pachytychius hordei hordei* (Brullé, 1832), *P. sparsutus* (Olivier, 1807)), Styphlini Jekel, 1861 (*Pseudostyphlus pillumus* (Gyllenhal, 1835), *Trachystyphlus beigerae* (Smreczyński, 1975)).

We studied both sexes of well-preserved, mature adult specimens. External characters were always examined in male specimens. All measurements were made under a stereomicroscope (Intraco Micro NSZ-810) using an ocular micrometer. Dissection of genitalia was carried out in both sexes after at least 24 h incubation in a wet chamber. Male genital structures were dissected and treated for five days in 10% KOH, which was then transferred to water and observed in glycerol. Female genitalia were studied, embedded in Solakryl BMX on a transparent plastic board. The hind wings of *A. histrio* were photographed embedded in Solakryl BMX, using a high-resolution camera (Canon EOS 50D) under the stereomicroscope in transmitted light. The spiculum ventrale (female eighth sternite) was mounted on a transparent board in Solakryl BMX and photographed under a laboratory microscope (Intraco Micro LMI T PC). Multilayer pictures were processed using the software Combine ZP.

The morphologic nomenclature was used according to the latest interpretation [5], following updates of the online glossary of weevil characters proposed in the International Weevils Community Website (18 February 2018) (http://weevil.info/glossary-weevil-characters) (accessed 14 March 2018).

The following abbreviations are used: Char. = character, n = not applicable.

2.2. Characters Used for Phylogenetic and Multi-Dimensional Phenetic Analyses

2.2.1. Morphological Characters

Morphological characters were selected *de novo* according to the aforementioned criteria and they were complemented by hind wing venation characters. The habitus of *Acentrus histrio* is shown in Figure 1.

Figure 1. *Acentrus histrio*. Male. According to [2]. (Not to scale). Copyright confirmed by M. Jäch (Koleopterologische Rundschau), 30 April 2018.

Char. 1: (0) eyes small to medium large, situated exclusively on lateral part of head; (1) eyes large, situated either only on lateral part of head or also partially on dorsal part of head, or medium large situated partially on dorsal part of head.

Char. 2: (0) head between eyes broad, of more than half of rostrum width at base; (1) head between eyes narrow, of at most half of rostrum width at base.

Char. 3: (0) distance between eyes larger or equal on ventral side of head than on forehead; (1) distance between eyes smaller on ventral side of head than on forehead.

Char. 4: (0) lower rostrum margin directed to inferior part of eye or below eye; (1) lower rostrum margin directed to middle of eye.

Char. 5: (0) antennal funicle with six or less segments or not differentiated from scape; (1) antennal funicle with seven segments.

Char. 6: (0) head and rostrum base dorsally bare or sparsely to semidensely, not confluently covered with hairs or scales, integument at least partially visible; (1) head and rostrum base covered with confluently densely arranged scales fully covering integument.

Char. 7: (0) antennal segment 1 bare or sparsely covered with hairs or seta-like scales; (1) antennal segment 1, at least in distal part densely covered with shortly elongated scales.

Char. 8: (0) lateral margin of mandibles with one or more large teeth; (1) lateral margin of mandibles without or with one small tooth or tubercle.

Char. 9: (0) lateral anterior margin of pronotum without postocular lobes; (1) lateral anterior margin of pronotum with postocular lobes.

Char. 10: (0) anterior margin of prosternum with no or shallow emargination, of less than 1/3 of the medial prosternal length; (1) anterior margin of prosternum with deep emargination, of at least 1/3 of the medial prosternal length.

Char. 11: (0) prosternum in medial part without impression along its whole medial length; (1) prosternum in medial part with impression along its whole medial length.

Char. 12: (0) mesoventral process markedly longer than wide at base; (1) mesoventral process at most as long as wide at base or slightly longer.

Char. 13: (0) distance between metacoxal apices less than twice as long as distance between precoxal apices; (1) distance between metacoxal apices twice as long or more as distance between precoxal apices.

Char. 14: (0) medial length of ventrite 1 shorter or equal to medial length of ventrite 2; (1) medial length of ventrite 1 longer than medial length of ventrite 2.

Char. 15: (0) medial length of ventrite 2 shorter or of the same length as medial length of ventrites 3–4 combined; (1) medial length of ventrite 2 longer than medial length of ventrites 3–4 combined.

Char. 16: (0) claws free; (1) claws at least at base connate.

Char. 17: (0) parameres absent, rudimentary in form of tubercles, "brush-like", transformed to plates or connate in their whole length; (1) parameres present, separated or connate only in basal part.

Char. 18: (0) tegmen oval to markedly elongated, always closed; (1) tegmen round, subround or moderately elongated, closed or open [6].

Char. 19: (0) manubrium tegmeni short to medium length, at most as long as longitudinal diameter of tegmen; (1) manubrium tegmeni long, longer than longitudinal diameter of tegmen [6].

Char. 20: (0) temones longer than median lobe; (1) temones shorter or equally as long as median lobe or rudimentary [6].

Char. 21: (0) intertemonal sclerites absent; (1) intertemonal sclerites present.

Char. 22: (0) saccus internus in median lobe without sclerites or sclerotized ductus; (1) saccus internus in median lobe with sclerites or sclerotized ductus.

Char. 23: (0) spiculum ventrale without arch-like arms; (1) spiculum ventrale with two arch-like arms and developed apodeme (Figure 2).

Figure 2. Spiculum ventrale (female eighth sternite) of *Acentrus histrio*. "Arch"-like arms (**a**), apodeme (**b**). (Not to scale).

Char. 24: (0) spermatheca simple, strongly sclerotized, not transparent, U-shaped, with almost undistinguishable corpus and cornu; (1) spermatheca more or less differentiated, moderately to slightly sclerotized, semi-transparent, with distinguishable corpus and cornu.

Char. 25: (0) ramus of spermatheca absent; (1) ramus of spermatheca present.

Char. 26: (0) nodulus of spermatheca present; (1) nodulus of spermatheca absent.

Char. 27: (0) cornu of spermatheca long, of more than maximal diameter of corpus; (1) cornu of spermatheca short, not longer than maximal diameter of corpus.

Char. 28: (0) hind wings absent or brachypterous; (1) hind wings fully developed.

Char. 29: (0) radial tending zone of hind wings long, of at least 0.45 wing length; (1) radial tending zone of hind wings short, of less than 0.45 wing length (Figure 3).

Figure 3. Hind wing of *Acentrus histrio*. Lateral sclerotized plate (SPl), radio-medial loop (R–M loop), radius posterior 2 (RP2), r4 vein (r4). (Not to scale).

Char. 30: (0) hind wings with well-developed RP2 (radius posterior); (1) hind wings with no or indistinct RP2 (Figure 3).

Char. 31: (0) radial cell (RC) of hind wings developed; (1) radial cell (RC) of hind wings absent (Figure 3).

Char. 32: (0) central field of hind wings with no or indistinct lateral sclerotized plate (SPl); (1) central field of hind wings with well-developed SPl (Figure 3).

Char. 33: (0) R–M loop of hind wings feebly visible or missing, r4 indistinct or missing; (1) R–M loop of hind wings well developed, r4 clearly visible (Figure 3).

Char. 34: (0) apical blood sinus ("pterostigma") clearly visible; (1) apical blood sinus ("pterostigma") absent or indistinct (Figure 3).

2.2.2. Host Plant Characters

Char. 35: (0) host plants not Eudicots [7]; (1) host plants Eudicots.
Char. 36: (0) host plants not Ranunculares [7]; (1) host plants Ranunculares.
Char. 37: (0) host plants Superrosids [7]; (1) host plants not Superrosids.
Char. 38: (0) host plants Superasterids [7]; (1) host plants not Superasterids.

2.3. Phylogenetic and Multi-Dimensional Phenetic Methods

Phylogenetic analyses were conducted on the data set (Table 1) comprising 34 morphological characters (characters 1–34) and four extrinsic characters concerning the host plants and their phylogenetic relationships [7]. All character states were unordered and unweighted except for characters 7, 14–16, 30, 32, 33, which were double-weighted, characters 2, 8, 11, 13, 18, 21, 23, 29, 36, which were triple-weighted and characters 1, 3, 4, 12, 17, 24, 31, which had a weight of 5. The weighting of the characters reflected their assumed taxonomic importance.

Phylogenetic trees were computed in maximum parsimony and Bayesian frameworks. The most parsimonious tree was found in PAUP* ver. 4.0b8 [8] using a heuristic search and 10 random addition species replicates. The accelerated transformation (ACCTRAN) optimization algorithm as well as the three bisection–reconnection (TBR) branch-swapping algorithm were applied. The reliability of its branching pattern was assessed using the bootstrap method with 100 replicates. Phylogenetic relationships were reconstructed also using Bayesian inference in the computer program MrBayes ver. 3.2.1 [9]. Bayesian analyses were conducted with the standard discrete evolutionary model and symmetric Dirichlet distribution for state rate variation among characters. The standard discrete model is analogous to the Jukes–Cantor evolutionary model in that any particular change from one state to another is equally probable, but has a variable number of states as it is in the one-parameter Markov k-state model. Two parallel runs with four chains were performed as part of the Markov chain Monte Carlo simulations. Posterior probabilities of the branching pattern were estimated from one million generations and trees sampled every 100 generations. The first 25% of sampled trees were discarded before constructing the 50% majority-rule consensus tree and calculating its posterior probabilities. Stationarity in the Bayesian analyses was confirmed in that the average standard deviation of the split frequencies was well below 0.01, the potential scale reduction factor approached 1, and no obvious trends were in the plots of generation vs. log probability.

The evolutionary history of all characters was reconstructed using the most parsimonious tree inferred from the matrix in Table 1 and the parsimony ancestral character state reconstruction method implemented in Mesquite ver. 3.40 [10].

The similarity of the analyzed taxa was assessed by nonmetric multi-dimensional scaling, as implemented in the scikit-learn ver. 0.19.1 package in Python [11]. When a character was not applicable to at least one taxon, it was excluded from the analysis. The SMACOF algorithm was run with 1000 initializations, each run had 20,000 iterations, and ε was set to 1×10^{-8} to declare convergence.

Table 1. Character matrix of tribes of the family Curculionidae ordered alphabetically and one outgroup species of the family Attelabidae.

Family	Subfamily	Tribe	Species	1	2	3	4	5	6	7	8	9	0	1	2	3	4	5	6	7	8	9	0	1	2	3	4	5	6	7	8	9	0	1	2	3	4	5	6	7	8
													Character No. (1)										(2)										(3)								
Attalabidae	Rhynchitinae	Rhynchitini	*Rhynchites bacchus*	0	0	0	0	0	0	0	0	0	0	0	0	0	1	0	0	0	0	0	0	0	0	0	0	0	0	1	1	1	0	0	0	1	1	1	0	0	1
Curculionidae	Brachycerinae	Erirhinini	*Notaris scirpi*	1	0	0	0	1	0	0	0	1	0	0	0	0	1	1	0	0	0	0	0	0	0	1	1	1	1	1	0	1	1	1	1	1	1	0	0	1	1
Curculionidae	Brachycerinae	Erirhinini	*Thryogenes fiorii*	1	0	0	0	1	0	0	0	0	0	0	0	0	1	1	0	0	0	0	0	0	0	1	1	1	1	1	0	n	n	n	n	n	n	0	0	1	1
Curculionidae	Brachycerinae	Erirhinini	*Thryogenes scirrhosus*	1	0	0	0	1	0	0	0	0	0	0	0	0	1	1	0	0	0	0	0	0	0	1	1	1	1	1	0	1	1	1	1	1	1	0	0	1	1
Curculionidae	Curculioninae	Acentrusini	*Acentrus histrio*	1	0	1	1	1	1	1	1	1	1	1	1	1	1	1	1	0	1	1	1	1	1	1	1	1	1	1	1	1	1	1	1	1	1	1	1	1	1
Curculionidae	Curculioninae	Acentrusini	*Acentrus zarathustra*	1	0	1	1	1	1	1	1	1	1	1	1	1	1	1	1	0	1	1	1	1	1	1	1	1	1	1	1	1	1	1	1	1	1	1	1	1	1
Curculionidae	Curculioninae	Anthonomini	*Anthonomus behnei*	1	0	0	0	0	0	0	1	0	0	0	1	0	1	0	0	0	1	1	1	0	0	0	1	0	1	0	1	0	0	1	1	0	0	1	0	0	1
Curculionidae	Curculioninae	Anthonomini	*Bradybatus seriesetosus*	1	0	0	0	0	0	0	1	0	1	0	1	0	1	0	1	0	1	1	1	0	0	0	1	0	1	0	1	0	0	1	1	0	0	1	0	0	1
Curculionidae	Curculioninae	Ellescini	*Dorytomus taeniatus*	1	1	0	0	1	0	0	1	0	0	0	1	0	1	0	0	1	1	1	0	0	1	0	1	1	1	1	1	1	0	1	1	0	0	1	0	0	1
Curculionidae	Curculioninae	Ellescini	*Ellescus bipunctatus*	1	1	0	0	1	0	0	1	0	1	1	1	0	1	0	0	1	1	1	1	0	1	0	1	1	0	0	1	1	0	1	1	0	1	1	0	0	1
Curculionidae	Curculioninae	Smicronychini	*Sharpia* sp.	1	0	1	1	1	1	0	1	0	1	0	1	1	1	1	1	1	1	1	1	0	1	0	1	1	1	0	1	1	1	1	1	1	0	1	0	0	1
Curculionidae	Curculioninae	Smicronychini	*Smicronyx jungermanniae*	1	0	1	1	1	0	0	1	1	1	1	1	1	1	1	1	1	1	1	1	0	0	0	1	0	1	1	1	1	0	1	1	1	1	1	0	1	0
Curculionidae	Curculioninae	Smicronychini	*Smicronyx reichii*	1	0	1	1	1	0	0	1	1	1	1	1	1	1	1	1	1	1	1	1	0	0	0	0	1	0	1	0	1	1	0	1	1	1	1	1	0	1
Curculionidae	Curculioninae	Storeini	*Pachytychius sparsutus*	1	0	0	0	1	0	0	1	0	1	0	0	0	1	1	0	1	1	0	1	0	0	0	1	1	1	0	1	0	1	1	1	1	0	1	0	0	1
Curculionidae	Curculioninae	Storeini	*Pachytychius hordei*	1	0	0	0	1	0	0	0	0	0	0	0	0	1	1	0	1	1	1	1	0	0	0	1	1	0	0	0	n	n	n	n	n	n	0	0	1	1
Curculionidae	Curculioninae	Styphlini	*Trachystyphlus beigerae*	1	0	1	0	1	0	0	1	1	1	0	0	1	1	0	0	0	1	1	1	1	0	0	1	1	1	0	0	n	n	n	n	n	n	1	0	1	0
Curculionidae	Curculioninae	Styphlini	*Pseudostyphlus pillumus*	1	0	1	0	1	1	0	1	0	1	0	0	0	1	0	0	0	1	1	0	1	0	0	1	1	1	0	1	1	1	1	1	1	1	1	0	1	0

3. Results and Discussion

The weighted maximum parsimony analysis revealed only a single most parsimonious tree with a length of 161 steps, a consistency index of 0.56 and a retention index of 0.77. The 50% majority-rule consensus tree inferred by Bayesian inference had a branching pattern identical to the most parsimonious tree and therefore posterior probabilities were mapped onto it along with maximum parsimony bootstrap values (Figure 4). Morphological character changes were also mapped on the most parsimonious tree (Figure 5). Interestingly, although multi-dimensional scaling is a phenetic method based only on similarity, the results were fully consistent with clades inferred by phylogenetic techniques (Figure 6). Taking into account the results of both phylogenetic and phenetic analyses, we assumed that the similarity of the weevil tribes in terms of the studied characters also reflected their phylogenetic relatedness.
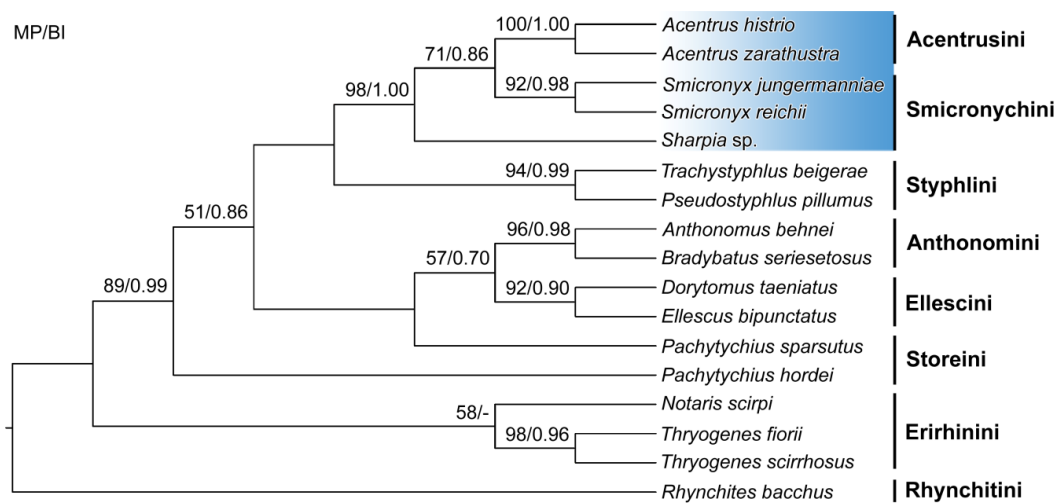
Figure 4. Weighted most parsimonious tree inferred from 38 characters of 16 species belonging to seven tribes of the family Curculionidae and one outgroup species (*Rhynchites bacchus*). The tree was constructed with the maximum parsimony method using PAUP*. Nodal supports are indicated as maximum parsimony (MP) bootstrap values in % and posterior probabilities for the Bayesian inference (BI). A dash indicates support below 0.50. Nodes without statistical support were not recognized in Bayesian and MP bootstrap analyses.

Smicronychini were recognized as the most closely phylogenetically-related tribe to Acentrusini. The monophyletic origin of the Smicronychini–Acentrusini group was supported by 98% maximum parsimony bootstrap and a posterior probability of 1.00 in the Bayesian tree (Figure 4). Likewise, Acentrusini and Smicronychini formed the most distinct cluster in the ordination diagram of nonmetric multi-dimensional scaling (Figure 6). Smicronychini, represented in this study by two species of *Smicronyx* and one species of *Sharpia*, were however depicted as a paraphyletic tribe encompassing Acentrusini in the phylogenetic trees. Specifically, *Smicronyx* was classified as a sister taxon of *Acentrus* with medium (71% bootstrap) to poor (posterior probability 0.86) statistical support (Figure 4). On the other hand, after nonmetric, multi-dimensional scaling, Smicronychini and Acentrusini each formed a homogenous group, corroborating the validity and distinctness of both tribes (Figure 6).
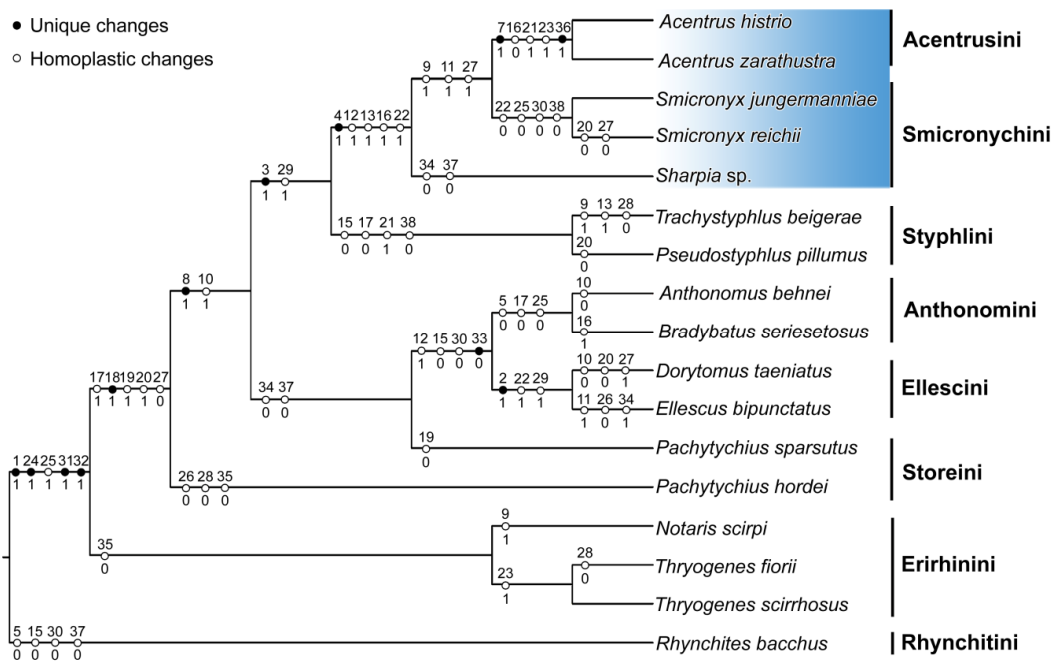
Figure 5. Evolution of character states in seven tribes of the family Curculionidae and one outgroup species (*Rhynchites bacchus*). Changes in character states were mapped on the most parsimonious tree shown in Figure 4, using the parsimony reconstruction method implemented in Mesquite. Black dots indicate unique character changes, while white dots indicate homoplastic changes.

In accordance with the current taxonomic concept, all other tribes of Curculioninae, except for Storeini, were revealed to be monophyletic, usually with strong statistical support. Thus, only the node separating members of Storeini was very poorly statistically supported (51% MP bootstrap and 0.86 posterior probability). Hence, the monophyly of *Pachytychius* species could also not be excluded. The monophyletic origin of the subfamily Curculioninae was well corroborated, while the subfamily Brachycerinae, represented here by the tribe Erirhinini, was only weakly statistically supported (58% MP bootstrap and posterior probability below 0.50) (Figure 4). The clusters recognizable in the ordination diagram were also basically consistent with and supported the current taxonomic concept (Figure 6).

The close phylogenetic relationship of Acentrusini and Styphlini proposed by Alonso-Zarazaga [1] was only partially confirmed by the present phylogenetic and multi-dimensional phenetic analyses. Similarly, the other supposedly related tribe Storeini is even less related to Acentrusini than Styphlini. Moreover, Storeini are presently regarded as a disputable tribe. Two Palaearctic genera, *Pachytychius*, included in this study, and *Aubeonymus* Jaquelin du Val, 1855, are considered genera *incertae sedis* [3]. According to the newest higher taxonomy concept, the tribe is treated as "*sensu lato*" [4]. The paraphyly of this tribe, revealed in this study (Figure 4), also reflects these doubts about the common origin of Storeini. On the other hand, the grouping of Acentrusini and Smicronychini was consistently recognized in all our analyses. Their most important apomorphy is the lower rostrum margin directed to the middle of the eye (char. 4). Styphlini is part of the clade that unites Acentrusini and Smicronychini, with a smaller ventral interocular distance (char. 3). However, the difference between the dorsal and the ventral interocular distance is not so strikingly expressed in Styphlini as it is in Acentrusini and Smicronychini. Despite the relatively small number of apomorphies in the cladogram (Figure 5), at least one apomorphy was found for almost each clade. For instance, the feebly visible R-M loop and r4 (char. 33) is synapomorphic for the tribes Anthonomini and Ellescini. The latter tribe is, in addition, characterized by an unequivocal apomorphy, with a narrow head between eyes (char. 2).
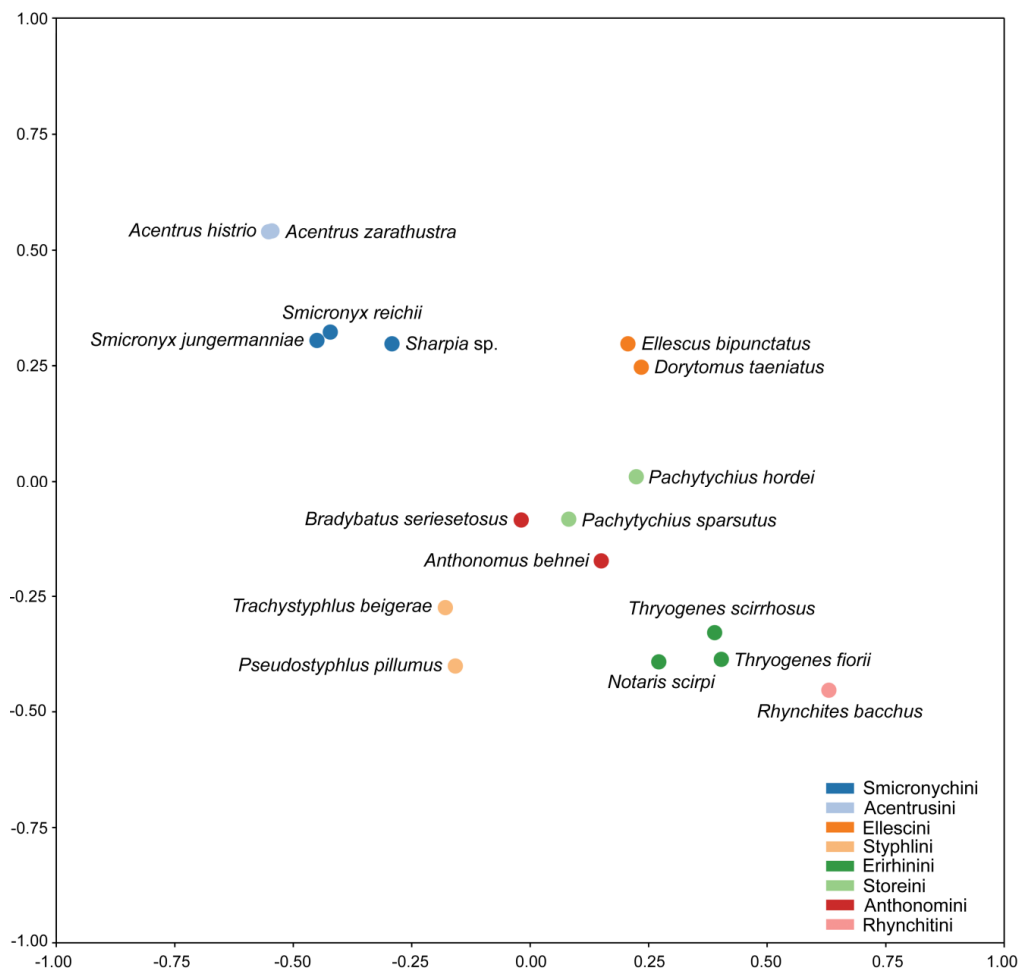
Figure 6. Nonmetric multi-dimensional scaling of 16 species belonging to seven tribes of the family Curculionidae and one outgroup species (*Rhynchites bacchus*). The ordination diagram was constructed from 32 characters, using the scikit-learn package in Python.

4. Conclusions

The weighted cladistic and multi-dimensional phenetic analyses showed that Smicronychini is the most closely related tribe to Acentrusini. On the other hand, Styphlini and Storeini were shown to be relatively unrelated to Acentrusini.

References

1.　Alonso-Zarazaga, M.A. Diagnosis preliminares de nuevos táxones de Curculionidae (Coleoptera). *Bol. SEA* **2005**, *37*, 89–93.

2.　Košťál, M. Revision of the genus *Acentrus* Desmarest, 1839 (Coleoptera: Curculionidae). *Koleopt. Rdsch.* **2014**, *84*, 329–336.

3. Caldara, R.; Franz, N.M.; Oberprieler, R.G. Curculioninae Latreille, 1802: Introduction, Phylogeny. In *Handbook of Zoology Volume 3*; Leschen, R.A.B., Beutel, R.G., Eds.; Walter de Gruyter GmbH: Berlin, Germany; Boston, MA, USA, 2014; Volume 3, pp. 589–628.

4. Alonso–Zarazaga, M.A.; Barrios, H.; Borovec, R.; Bouchard, P.; Caldara, R.; Colonnelli, E.; Gültekin, L.; Hlaváč, P.; Korotyaev, B.; Lyal, C.H.C.; et al. *Cooperative Catalogue of Palaearctic Coleoptera Curculionoidea*; Monografias Electrónicas SEA 8. Sociedad Entomológica Aragonesa, S.E.A.: Zaragosa, Spain, 2017; p. 729.

5. Oberprieler, R.G.; Anderson, R.S.; Marvaldi, A.E. Curculionoidea Latreille, 1802: Introduction, Phylogeny. In *Handbook of Zoology Volume 3*; Leschen, R.A.B., Beutel, R.G., Eds.; Walter de Gruyter GmbH: Berlin, Germany; Boston, MA, USA, 2014; Volume 3, pp. 285–300.

6. Košťál, M.; Košťálová, Z. Description of the male of *Acentrus boroveci* Košťál, 2014 (Coleoptera: Curculionidae: Acentrusini). *Zootaxa* **2016**, *4121*, 77–80. [CrossRef] [PubMed]

7. Byng, J.W.; Chase, M.W.; Christenhusz, M.J.M.; Fay, M.F.; Judd, W.S.; Mabberley, D.J.; Sennikov, A.N.; Soltis, D.E.; Soltis, P.S.; Stevens, P.F.; et al. An update of the Angiosperm Phylogeny Group classification for the orders and families of flowering plants: APG IV. *Bot. J. Linn. Soc.* **2016**, *181*, 1–20.

8. Swofford, D.L. PAUP*. In *Phylogenetic Analysis Using Parsimony (*and Other Methods)*, version 4; Sinauer Associates: Sunderland, MA, USA, 2002; p. 144.

9. Ronquist, F.; Teslenko, M.; van der Mark, P.; Ayres, D.L.; Darling, A.; Höhna, S.; Larget, B.; Liu, L.; Suchard, M.A.; Huelsenbeck, J.P. MrBayes 3.2: Efficient Bayesian phylogenetic inference and model choice across a large model space. *Syst. Biol.* **2012**, *61*, 539–542. [CrossRef] [PubMed]

10. Maddison, W.P.; Maddison, D.R. Mesquite: A Modular System for Evolutionary Analysis. Version 3.40. Available online: http://mesquiteproject.org (accessed on 30 April 2018).

11. Pedregosa, F.; Varoquaux, G.; Gramfort, A.; Michel, V.; Thirion, B.; Grisel, O.; Blondel, M.; Prettenhofer, P.; Weiss, R.; Dubourg, V.; et al. Scikit-learn: Machine learning in Python. *J. Mach. Learn. Res.* **2011**, *12*, 2825–2830.